JOURNAL OF VIROLOGY, Aug. 2009, p. 8233–8246 Vol. 83, No. 16
0022-538X/09/$08.00+0 doi:10.1128/JVI.02672-08

Lack of Bax Prevents Influenza A Virus-Induced Apoptosis and Causes Diminished Viral Replication▽

Jeffrey E. McLean, Emmanuel Datan, Demetrius Matassov,† and Zahra F. Zakeri*

Department of Biology, Queens College and Graduate Center of the City University of New York, Flushing, New York 11367

Received 29 December 2008/Accepted 18 May 2009

The ectopic overexpression of Bcl-2 restricts both influenza A virus-induced apoptosis and influenza A virus replication in MDCK cells, thus suggesting a role for Bcl-2 family members during infection. Here we report that influenza A virus cannot establish an apoptotic response without functional Bax, a downstream target of Bcl-2, and that both Bax and Bak are directly involved in influenza A virus replication and virus-induced cell death. Bak is substantially downregulated during influenza A virus infection in MDCK cells, and the knockout of Bak in mouse embryonic fibroblasts yields a dramatic rise in the rate of apoptotic death and a corresponding increase in levels of virus replication, suggesting that Bak suppresses both apoptosis and the replication of virus and that the virus suppresses Bak. Bax, however, is activated and translocates from the cytosol to the mitochondria; this activation is required for the efficient induction of apoptosis and virus replication. The knockout of Bax in mouse embryonic fibroblasts blocks the induction of apoptosis, restricts the infection-mediated activation of executioner caspases, and inhibits virus propagation. Bax knockout cells still die but by an alternative death pathway displaying characteristics of autophagy, similarly to our previous observation that influenza A virus infection in the presence of a pancaspase inhibitor leads to an increase in levels of autophagy. The knockout of Bax causes a retention of influenza A virus NP within the nucleus. We conclude that the cell and virus struggle to control apoptosis and autophagy, as appropriately timed apoptosis is important for the replication of influenza A virus.

The pathology of influenza A virus infection usually arises from acute lymphopenia and inflammation of the lungs and airway columnar epithelial cells (23, 38). Influenza A virus induces apoptotic death in infected epithelial, lymphocyte, and phagocytic cells, and apoptosis is a source of tissue damage during infection (3, 22, 33) and increased susceptibility to bacterial pathogens postinfection (31). While the induction of apoptosis by influenza A virus has been well documented (4, 19–21, 28, 33, 37), the mechanisms of this interaction are not well understood. Two viral proteins, NS1 and PB1-F2, have been associated with viral killing of cells. NS1, originally characterized as being proapoptotic (34), was later identified as being an interferon antagonist, inhibiting the activation of several key antiviral responses and restricting the apoptotic response to infection (1, 10, 15, 18, 35, 39, 46). In contrast, PB1-F2 induces apoptosis primarily by localizing to the outer mitochondrial membrane, promoting cytochrome *c* release, and triggering the apoptotic cascade (43). This effect, however, is typically restricted to infected monocytes, leading to the hypothesis that PB1-F2 induces apoptosis specifically to clear the landscape of immune responders (5, 44). Although PB1-F2 activity does not directly manipulate virus replication or virus-induced apoptosis, PB1-F2 localization to the mitochondrial membrane during infection potentiates the apoptotic response in epithelial and fibroblastic cells through tBID signaling with proapoptotic Bcl-2 family protein members Bax and Bak (22, 43, 44).

The Bcl-2 protein family consists of both pro- and antiapoptotic members that regulate cytochrome *c* release during mitochondrion-mediated apoptosis through the formation of pore-like channels in the outer mitochondrial membrane (12, 16). During the initiation of mitochondrion-mediated apoptosis, cytoplasmic Bid is cleaved to form tBID. This, in turn, activates proapoptotic Bax and Bak (40), which drive cytochrome *c* release and subsequent caspase activation. Bak is constitutively associated with the mitochondrial membrane, whereas inactive Bax is primarily cytosolic, translocating to the outer mitochondrial membrane only after activation (6). The activation of Bax and Bak results in homo- and heterodimer formation at the outer mitochondrial membrane, generating pores that facilitate mitochondrial membrane permeabilization and cytochrome *c* release (14, 17), leading to caspase activation and the apoptotic cascade (8). Antiapoptotic members of the Bcl-2 protein family, including Bcl-2, inhibit the activation of proapoptotic Bax and Bak primarily by sequestering inactive Bax and Bak monomers via interactions between their BH3 homology domains (7).

Bcl-2 expression has been linked to decreased viral replication rates (26). Bcl-2 overexpression inhibits influenza A virus-induced cell death and reduces the titer and spread of newly formed virions (29). The activation of caspase-3 in the absence of sufficient Bcl-2 is critical to the influenza A virus life cycle. Both Bcl-2 expression and the lack of caspase activation during infection lead to the nuclear accumulation of influenza virus ribonucleoprotein (RNP) complexes, thereby leading to the improper assembly of progeny virions and a marked reduction in titers of infectious virus (26, 41, 42, 45).

* Corresponding author. Mailing address: Queens College of the City University of New York, 65-30 Kissena Blvd., Flushing, NY 11367. Phone: (718) 997-3417. Fax: (718) 997-3429. E-mail: zahra_zakeri@hotmail.com.

† Present address: Division of Vaccine Vectors, Profectus BioSciences, Tarrytown, NY 10591.

▽ Published ahead of print on 3 June 2009.

Here we show that influenza A virus induces mitochondrion-mediated (intrinsic-pathway) apoptosis signaled specifically through Bax and that this Bax signaling is essential for the maximum efficiency of virus propagation. In contrast, Bak expression is strongly downregulated during infection. Cells lacking Bak (while expressing Bax) display a much more severe apoptotic phenotype in response to infection and produce infectious virions at a higher rate than the wild type (WT), suggesting that Bak, which can suppress viral replication, is potentially downregulated by the virus. Our results indicate essential and opposing roles for Bax and Bak in both the response of cells to influenza A virus infection and the ability of the virus to maximize its own replicative potential.

MATERIALS AND METHODS

Cell culture and experimental treatment. MDCK cells were supplied by Anastasia Gregoriades, Queens College, Queens, NY. Simian virus 40-immortalized, adherent WT, $Bax^{-/-}$ (Bax knockout [KO]), $Bak^{-/-}$ (Bak KO), and Bax/Bak double-KO (DKO) mouse embryonic fibroblasts (MEFs) were a generous gift of the late Stanley Korsmeyer of Harvard University, Boston, MA. All cells were maintained in Dulbecco's modified Eagle medium (DMEM) (catalog no. 12800-017; Gibco) supplemented with 10% heat-inactivated fetal bovine serum (ΔFBS) (catalog no. LSFB-0500; Equitech-Bio), 2 mM L-glutamine (catalog no. 25030-081; Gibco), 1.5 g/liter sodium bicarbonate (Sigma-Aldrich, St. Louis, MO), and 50 U/ml penicillin plus 50 mg/ml streptomycin (catalog no. 15140-122; Gibco) and incubated at 37°C under a humidified 5% CO_2 atmosphere. All experiments were run in triplicate. For all experiments except plaque assay, exponentially growing cells were seeded at 4×10^5 cells per plate and allowed to attach overnight before influenza A/WSN/33 virus was delivered to rinsed cells at a multiplicity of infection (MOI) of 5 for 1 h at room temperature (RT). The cells were covered with DMEM containing 5% ΔFBS, 50 U/ml penicillin, and 50 mg/ml streptomycin and incubated at 37°C until collection. Bax replacement in KO cells was achieved through the transient transfection of plasmid C2-Bax-GFP under the control of a human cytomegalovirus promoter (a generous gift of the late Stanley Korsmeyer, Harvard University) by use of Lipofectamine 2000 reagent (catalog no. 52887; Invitrogen) according to the manufacturer's protocol. In brief, plasmid DNA was mixed with Lipofectamine 2000 reagent and applied to cells for 4 h at 37°C. The cells were then rinsed, covered with DMEM containing 10% ΔFBS, and incubated at 37°C for 15 h before viral infection. A transfection efficiency of at least 50% was confirmed using fluorescence microscopy (data not shown).

Viral growth and titer determination. Influenza A/WSN/33 virus was cultured in 10-day-old specific-pathogen-free embryonated chicken eggs (Charles River SPAFAS, North Franklin, CT) for 2 days at 35°C. Infected egg albumen was collected and cleared by centrifugation at 1,000 rpm for 10 min. The supernatant was collected and stored at −80°C. Virus titer was determined by plaque assay. Briefly, monolayers of MDCK cells were incubated overnight in DMEM containing 10% ΔFBS and 1% penicillin-streptomycin. This was followed by infection with 10-fold serial dilutions of virus suspension for 1 h at RT. Cells were then covered with warmed Eagle's minimum essential medium (catalog no. 12-668E; BioWhittaker) containing 0.1% DEAE-dextran (catalog no. D9885; Sigma-Aldrich) and 1% purified agar (catalog no. LP0028; Oxoid). This agar medium was allowed to solidify at RT and incubated for 2 days at 37°C to promote plaque development. Immediately prior to plaque analysis, the solidified agar was removed, and cells were fixed and stained with a methanol-crystal violet solution. Plaques were counted, and the virus titer was expressed as PFU/ml. For experimental determinations of virus replication, cells were infected with influenza A/WSN/33 virus at an MOI of 0.01, and at 24-h intervals, cell supernatant samples were collected and plaques were assayed.

Assessment and characterization of cell death. The effect of Bax and Bak KO during influenza A virus-induced cell death was assessed using a trypan blue exclusion assay. Cells were infected with influenza A virus as described above and detached from culture plates by trypsin digestion. Washed cell pellets were resuspended in 1× phosphate-buffered saline (PBS), and samples were mixed 1:1 with 0.4% trypan blue (catalog no. 302643; Sigma-Aldrich) in 1× PBS solution and incubated at RT for 5 min. Trypan blue is taken up by dead cells and excluded from living cells by their intact cell membranes. Cells were counted by use of a hemocytometer. In all cases, percent cell death was calculated as the ratio of dead cells to the total number of cells. The percent cell death of mock-infected cells was subtracted as background, and data are expressed as percent cell death greater than death in mock-infected cells. The effect of Bax and Bak KO on Influenza A virus-induced cell death was further characterized by Hoechst staining, which is a reliable indicator of chromatin condensation and nuclear fragmentation, markers of mid- to late-stage apoptotic cell death. Cells were infected and collected as described above. Cell pellets were washed once with ice-cold 1× PBS and resuspended in ice-cold 3.5% paraformaldehyde (catalog no. 04042; Fisher) for 10 min. Fixed cells were stained on ice with 16 μg/ml Hoechst 33258 bis-benzimide stain (catalog no. 2883; Sigma-Aldrich) for 30 min, rinsed once with 1× PBS, and analyzed for chromatin condensation by fluorescence microscopy (Leitz, Germany). Healthy and apoptotic nuclei were counted, and in all cases, the count of mock-infected apoptotic nuclei was subtracted from the count of influenza A virus-infected apoptotic nuclei, and data are expressed as percent apoptotic nuclei greater than mock. Executioner caspase activity in mock- and influenza A virus-infected cells was quantified as the cleavage of fluorogenic caspase-3/7 substrate rhodamine 110, bis(*N*-carbobenzyloxy-L-aspartyl-L-glutamyl-L-valyl-L-aspartic acid amide [Z-DEVD-R110]), using the Apo-One homogenous caspase-3/7 assay kit (catalog no. G7792; Promega) according to the manufacturer's protocol.

Quantification of viral RNA release. The amount of total influenza A virus RNA released during infection in WT, Bax KO, Bak KO, and Bax/Bak DKO cells was determined by collecting cell supernatant samples at 48 h postinfection (hpi) and subjecting them to quantitative reverse transcription-PCR. Total viral RNA was extracted at 12 hpi and 24 hpi using a viral RNA extraction kit (catalog no. 52904; Qiagen) according to the manufacturer's protocol. cDNA was then generated from extracted viral RNA using a Superscript III first-strand synthesis kit (catalog no. 18080-400; Invitrogen) according to the manufacturer's protocol. One microgram of cDNA was amplified by quantitative reverse transcription-PCR in 20-μl reaction mixtures using a LightCycler FastStart DNA Master Sybr green 1 kit (catalog no. 03515869001; Roche) with forward primer TACACCC AGTCACAATAGGAGAGTG and reverse primer CCATGCATTCATTGTC ACACTTGTGG for the influenza A virus hemagglutinin (HA) gene using a Roche LightCycler 2.0 real-time PCR machine under the following conditions: 95°C for 10 min, followed by 50 cycles of 10 min at 95°C, 5 min at 69°C, and 22 min at 72°C. Samples of known viral titers were also analyzed to develop a standard curve of influenza A virus particles released/ml, to which experimental samples were normalized. Relative influenza A virus particle release in each cell type was compared to that for mock-infected cells and presented as a ratio of infected/mock-infected cells.

Assessment of the influenza A virus-induced interferon response. To determine the effect of Bax and/or Bak KO on influenza A virus-induced interferon signaling, cells were infected as described above. This was followed by secondary infection in both mock- and influenza A virus-infected cells at 24 hpi with green fluorescent protein (GFP)-tagged Newcastle disease virus (NDV) (provided by Adolfo Garcia-Sastre, Mt. Sinai University and Medical Center, New York, NY) at an MOI of 1 or 2. NDV-GFP is suppressed by interferon activity. Following secondary infection, cells were incubated for an additional 24 h at 37°C under a humidified 5% CO_2 atmosphere to allow NDV-GFP expression. Cells were then collected and immediately analyzed by fluorescence-activated cell sorter (FACS) analysis. An increase in interferon activity caused by the initial influenza A virus infection causes a corresponding decrease in the level of NDV-GFP expression, which can be quantified using FACS analysis as an indirect measure of interferon activity. The experiment was run in triplicate, and 10,000 events per sample were analyzed. Mean fluorescence was expressed as the ratio of infected to mock mean fluorescence.

Protein analysis and immunocytochemistry. For determinations of cytochrome *c* release in MDCK cells, mitochondria from mock- and influenza A virus-infected cells were separated from cells at 8, 12, 18, and 24 hpi by homogenization and differential centrifugation, and total protein lysates from both the cellular and mitochondrial fractions were isolated and analyzed by Western blotting. Bax and Bak expression profiles in MDCK cells were determined by collecting total protein lysates from mock- and influenza A virus-infected cells at 24 hpi and analyzing them by Western blotting using anti-Bax (catalog no. sc493; Santa Cruz Biotech) and anti-Bak (catalog no. sc832; Santa Cruz Biotech) antibodies. For determinations of apoptosis protein expression levels during infection of WT, Bax KO, Bak KO, and Bax/Bak DKO cells, protein expression profiles of mock- and influenza A virus-infected cells were obtained at 48 hpi to allow the full expression of response proteins during influenza A virus-induced cell death and analyzed by Western blotting. Cells were then scraped from the plates, and the cell pellet was resuspended in ice-cold radioimmunoprecipitation assay (RIPA) buffer (10 mM Tris-HCl [pH 7.4], 150 mM NaCl, 1% Triton X-100, 0.1% sodium dodecyl sulfate, 0.5 mM EDTA) containing a protease inhibitor cocktail (catalog no. 11836-170-001; Roche) and centrifuged for 10 min at 1,000 × *g* at

4°C. The supernatant was collected, transferred into a new ice-cold tube, and stored at −20°C. For determinations of influenza A virus nucleoprotein (NP) nuclear localization in WT, Bax KO, Bak KO, and Bax/Bak DKO cells, cells were infected at an MOI of 5 and collected by trypsin digestion at 24 hpi. Cells were then washed once with ice-cold 1× PBS, resuspended in hypotonic buffer (10 mM HEPES, 1.5 mM $MgCl_2$, 10 mM KCl, 0.5 mM dithiothreitol) containing a protease inhibitor cocktail (catalog no. 11836-170-001; Roche), and incubated on ice for 10 min to cause cell swelling. Cells were then burst using a Dounce homogenizer and centrifuged to obtain a nuclear pellet. The supernatant was collected as the cytoplasmic fragment, mixed with 5× RIPA buffer, and incubated on ice for 20 min. The nuclear pellet was resuspended in 0.25 M sucrose containing 10 mM $MgCl_2$ and layered over a 0.88 M sucrose cushion containing 10 mM $MgCl_2$, followed by centrifugation at 2,800 × *g*. The supernatant was aspirated, resuspended in 1× RIPA buffer, and vortexed on ice to release nuclear proteins, followed by incubation on ice for 20 min. Both cytoplasmic and nuclear fractions were then cleared of debris by centrifugation. The total protein content was determined using the Bio-Rad protein assay (catalog no. 500-0006).

For Western blot analysis, equal quantities of proteins (30 μg) were loaded onto a polyacrylamide gel and subjected to sodium dodecyl sulfate-polyacrylamide gel electrophoresis. Proteins were then transferred onto a nitrocellulose membrane (catalog no. RPN-303E; Amersham) overnight at 4°C. The nonspecific proteins were blocked using 4% milk solution and subjected to different primary antibodies: anti-cleaved caspase-7 (catalog no. 9491s; BD Pharmingen), anti-active caspase-3 (catalog no. 559565; Sigma), anti-Bcl-2 (catalog no. sc492; Santa Cruz Biotech), anti-influenza A virus NP (provided by Adolfo Garcia-Sastre, Mt. Sinai University and Medical Center), and anti-β-tubulin (catalog no. sc9104; Santa Cruz Biotech), which was used as a loading control. Positive signals were detected using ECF (catalog no. RPN5787; GE Healthcare) according to the manufacturer's protocol and visualized using a Storm 860 scanner and software (GMI, Inc., MN) or by ECL (catalog no. RPN2132; GE Healthcare) and visualized using Amersham Hyperfilm ECL photoradiographic film (catalog no. 28906835; GE Healthcare).

For immunocytochemical analysis, 4×10^5 cells were seeded onto heat-sterilized glass coverslips. After overnight incubation at 37°C, attached cells were carefully rinsed with 1× PBS and infected as described above. At 24 or 48 hpi, cells were fixed with ice-cold 3.5% paraformaldehyde for 10 min and rinsed with ice-cold 1× PBS. Nonspecific binding sites were blocked using 1× PBS containing 18 μg/ml bovine serum albumin before immunoblotting with the rabbit antibodies anti-Bax (catalog no. sc493; Santa Cruz Biotech), anti-active caspase-3 (catalog no. 559565; Sigma), anti-influenza A/WSN virus (provided by Adolfo Garcia-Sastre, Mt. Sinai University and Medical Center, New York, NY), or anti-influenza A virus NP. Cells were then rinsed three times in 1× PBS, followed by incubation with anti-rabbit immunoglobulin G-Alexa Fluor 488 secondary antibody (catalog no. A11008; Invitrogen) solution for 2 h. Cells were then rinsed twice with 1× PBS before staining polymerized actin with phalloidin-tetramethyl rhodamine isocyanate (phalloidin-TRITC; catalog no. P1951; Sigma) and before staining nuclei with 4′,6′-diamidino-2-phenylindole (DAPI) (catalog no. D8417; Sigma). Stained cells were then mounted using GelMount (catalog no. M-01; Biomeda) and visualized using a confocal microscope (Leica, Germany).

Determination of lysosomal localization and function. Cells were infected and fixed on slides as described above. Lysosomal localization was determined by staining cells with 1 μl/ml LysoTracker Red DND-99 (catalog no. L7528; Invitrogen) for 30 min immediately prior to fixation. Cells were then rinsed once with 1× PBS and fixed using ice-cold 3% paraformaldehyde in 1× PBS for 10 min. Nuclear localization was also determined by staining with 10 μg/ml of DAPI (catalog no. D8417; Sigma) for 10 min at RT prior to mounting. Cells were then mounted with gel mount (catalog no. M-01; Biomeda) and visualized by confocal microscopy (Leica, Germany).

For measurements of lysosomal activity, cells were infected and collected as described above. The activity of the lysosomal enzyme acid phosphatase was assessed using an acid phosphatase assay kit (catalog no. CS0740; Sigma) according to the manufacturer's protocol. Briefly, cells were infected as described above, rinsed once, and collected by scraping. A total of 10^6 cells from each sample were then resuspended in acid phosphatase substrate solution (*p*-nitrophenyl phosphate) for 30 min at RT. The reaction was stopped by the addition of a 0.5 N NaOH solution to the mixture, and the absorbance of each sample at 405 nm was measured spectrophotometrically with an Ultraspec III spectrophotometer (Pharmacia LKB, Sweden).

To determine the overall lysosomal volume of mock- and influenza A virus-infected cells, cells were infected as described above and incubated with 1 μl/ml LysoTracker Red DND-99 for 30 min immediately prior to collection. Cells were then rinsed once with 1× PBS and collected by trypsin digestion, followed by FACS analysis. The experiment was performed in triplicate, and 10,000 events per sample were analyzed. The mean fluorescences of both mock-infected and influenza A virus-infected samples were compared as an indicator of lysosomal staining intensity, a marker of lysosomal volume.

Determination of LC3 cleavage and translocation. To confirm the induction of an autophagy following influenza A virus infection in the absence of Bax, we assessed the localization of LC3 at 24 hpi. A total of 4×10^5 cells were plated onto heat-sterilized glass coverslips in 35-mm plates, and LC3-GFP was transiently expressed by transfection with a C1-LC3-GFP construct (provided by Guido Kroemer, Institut Gustave-Roussy, Villejuif, France) using Lipofectamine 2000 (catalog no. 52887; Invitrogen) and incubated for 16 h to allow LC3-GFP expression. Cells were then infected as described above. At 24 hpi, cells were fixed with ice-cold 3.5% paraformaldehyde (catalog no. 04042; Fisher) for 10 min and rinsed once with 1× PBS. Cells were then embedded by gel mount (catalog no. M-01; Biomeda) and observed by confocal microscopy. The generation of a punctate GFP expression pattern is indicative of LC3 translocation and autophagosome formation, which occurs exclusively during autophagy. A transfection efficiency of at least 50% was confirmed using fluorescence microscopy (data not shown). Mock-infected cells were also analyzed to ensure that LC3-GFP expression alone did not cause an autophagic response.

RESULTS

Influenza A virus infection induces apoptosis and disables mitochondrial function. Influenza A virus infection drives an apoptotic response in host cells (19–23, 28, 33, 36–45; A. Shirazian, D. Matassov, J. E. McLean, and Z. F. Zakeri, unpublished data). In an effort to understand if and how influenza A virus-induced apoptosis is affected by mitochondrion-driven apoptosis signaling, we initially used MDCK cells, which are both permissive to infection and highly susceptible to influenza A virus-induced killing. Cell death in response to influenza A virus infection was assessed initially by the trypan blue exclusion assay described in Materials and Methods. Subsequently, influenza A virus-induced death was characterized by several markers of apoptosis at different times postinfection. We concluded that the level of cell death measured by trypan blue was similar to that obtained by other markers and furthermore that cell death was apoptotic, consistent with findings reported previously by several other groups. As shown in Fig. 1A, by 24 hpi, more than 50% of influenza A virus-infected cells died, and by 48 hpi, 90% of infected cells died. Hoechst analyses examining the level of condensed and fragmented nuclei in infected cell populations showed that nuclear alterations typical of apoptosis followed a pattern consistent with death as measured by trypan blue (Fig. 1A). This indicates that influenza A virus-induced death is most likely apoptotic, a fact that was confirmed by the measurement of activation of caspase-3 (data not shown; Shirazian et al., unpublished).

One milestone during mitochondrion-mediated apoptosis is cytochrome *c* release from the inner mitochondrial space to the cytosol, where it activates apoptosis. This release is typically modulated by the activity of Bcl-2 family proteins and usually occurs without an immediate decline in the function of mitochondrial enzymes (7, 8, 11, 16, 40). We assessed the level of cytochrome *c* release in response to influenza A virus infection by the evaluation of the presence of cytochrome *c* in different cell fractions (i.e., the cytoplasmic versus mitochondrial fraction obtained by differential centrifugation of mock-infected and infected MDCK cells at various times postinfection). The presence of cytochrome *c* was evaluated and analyzed by Western blotting using anti-cytochrome *c* antibodies. The distribution of cytochrome *c* shifted dramatically from

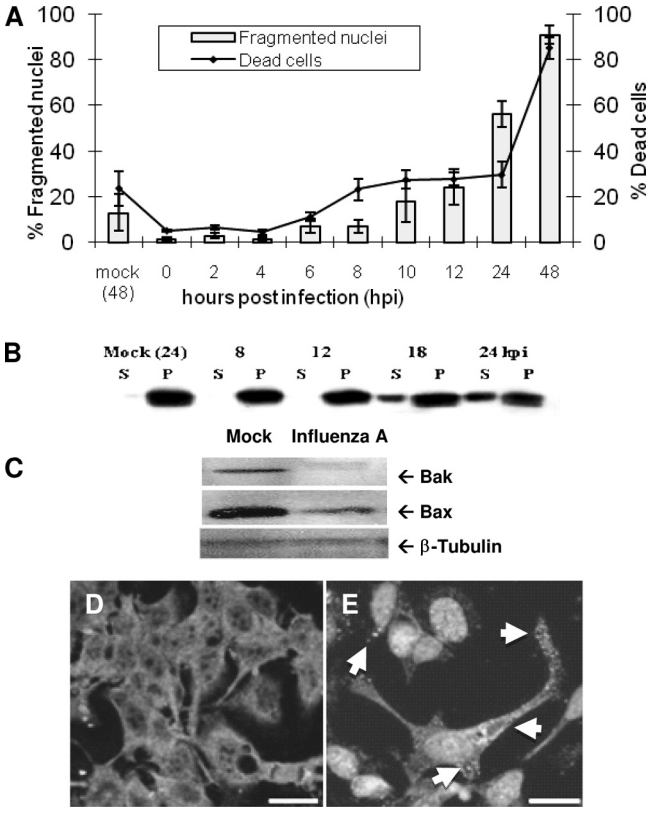

FIG. 1. Influenza A virus induces apoptosis through mitochondrial permeabilization via Bax activation. (A) Influenza A virus induction of MDCK cell death was assessed using trypan blue exclusion. Cell killing by influenza A/WSN/33 virus is pronounced by 24 hpi, with nearly total population death by 48 hpi (right axis, line). Nuclear alterations typical of apoptosis were observed by Hoechst staining and fluorescence microscopy. Dramatic nuclear fragmentation was seen by 24 hpi, and almost all cells exhibited nuclear fragmentation by 48 hpi (left axis, bars), indicating that influenza A virus-induced cell death is primarily apoptotic. (B) Cytochrome *c* release was assessed by centrifugal separation of mitochondria from the cytoplasm followed by Western blotting for cytochrome *c*. Cytochrome *c* was seen to shift from an exclusively mitochondrial localization (P) to the cytosolic compartment (S) by 18 hpi. (C) Bax and Bak expression in MDCK cells following infection was assessed by Western blotting. Bak, a protein that constitutively associates with the outer mitochondrial membrane, is severely downregulated following infection in MDCK cells. Bax is slightly downregulated by 24 hpi. β-Tubulin was used as a loading control. (D and E) Bax activation and translocation were assessed by immunocytochemistry and confocal microscopy. (D) Mock-infected cells show a diffuse staining pattern indicating inactive Bax located throughout the cytoplasm. (E) Upon activation by influenza A virus, Bax was seen to shift from its inactive cytoplasmic distribution to a punctate distribution (arrows) as activated Bax was translocated to the mitochondria following infection. In this figure, DAPI rather than Bax stains the nuclei. Bars, 50 μm.

the pelleted, mitochondrial fraction to the soluble, cytoplasmic fraction as early as 18 hpi; this distribution was maintained through 24 hpi (Fig. 1B).

Bax and Bak form cytochrome *c* release channels in the outer mitochondrial membrane, allowing cytochrome *c* release to the cytosol. We therefore assessed the levels of Bax and Bak expression in mock-infected and infected MDCK cells at 24 hpi. β-Tubulin was used as a loading control. As shown in Fig. 1C, Bax expression was downregulated, while Bak expression almost totally disappeared after influenza A virus infection.

Bax and Bak are considered to be proapoptosis partners during intrinsic pathway signaling (7), acting in tandem to induce cytochrome *c* release and subsequent caspase activation. As Bax, but not Bak, expression is still evident in infected cell populations, we assessed the localization of Bax at 24 hpi by using a Bax-specific antibody and confocal microscopy. A diffuse cytoplasmic distribution of Bax, typical of inactive Bax in healthy cells, was found in the mock-infected cells (Fig. 1D). In contrast, infected cells showed a punctate Bax staining pattern, which is typical of Bax activation in cells undergoing an apoptotic response, as reported previously (11, 41) (Fig. 1E). (The appearance of nuclear localization is due to DAPI staining in these pictures.) These results suggest that the apoptotic response generated by influenza A virus infection is due to Bax-mediated cytochrome *c* release and that Bak is actively downregulated by the virus during infection. The observed elimination of Bak and activation (movement to mitochondria) of Bax during infection suggest that Bax, but not Bak, is important for the efficient induction of death by influenza A virus during infection.

Bax KO inhibits, while Bak KO potentiates, influenza A virus-induced mitochondrion-mediated apoptosis. Our findings that Bax and Bak activities are differently affected by influenza A virus infection prompted us to further explore the activities of these two proteins during influenza A virus-induced cell killing. We used C57Black, simian virus 40-immortalized MEFs that were WT or that possessed a genetic KO of Bax, Bak, or both (40). We infected WT, Bax KO, Bak KO, and Bax/Bak DKO cells with influenza A virus and assessed the level of cell death after 24 and 48 hpi. As shown in Fig. 2A, while the death rates of infected Bax KO cells do not differ from those of the WT, the rate of death of Bak KO cells is markedly higher than that of WT cells at both 24 hpi ($P < 0.0001$) and 48 hpi ($P < 0.0002$). These results suggest that influenza virus requires neither Bax nor Bak to kill the cells, that the cells are more vulnerable when Bax is present in the absence of Bak, and that Bax is required for death to be apoptotic. The increase over the control in rates of death observed in Bax/Bak DKO cells at both 24 hpi ($P < 0.03$) and 48 hpi ($P < 0.000002$) suggests that the virus can trigger alternate death pathways that are otherwise not seen when both of these proapoptotic proteins are present.

To assess the amount of apoptosis in response to influenza A virus under each KO condition, we first quantified the numbers of condensed and fragmented nuclei at 24 hpi and 48 hpi using Hoechst staining. The increase in numbers of fragmented nuclei in WT, Bak KO, and Bax/Bak DKO correlates with the levels of cell death following infection (Fig. 2B). However, Bax KO cells, which experience rates of death very similar to those of the WT after infection, develop almost no fragmented nuclei compared to the WT at both 24 hpi ($P < 0.00003$) and 48 hpi ($P < 0.0002$). Influenza A virus-induced changes in nuclear morphology are increased in Bak KO cells compared to those of WT cells at 24 hpi ($P = 0.04$) and 48 hpi ($P < 0.0002$). At 24 hpi, mock-infected cells of all types manifest primarily healthy nuclei (Fig. 2C to F). Influenza A virus-infected WT, Bak KO, and DKO cells manifest many condensed and fragmented nuclei (Fig. 2G, H, and J). However, Bax KO cells,

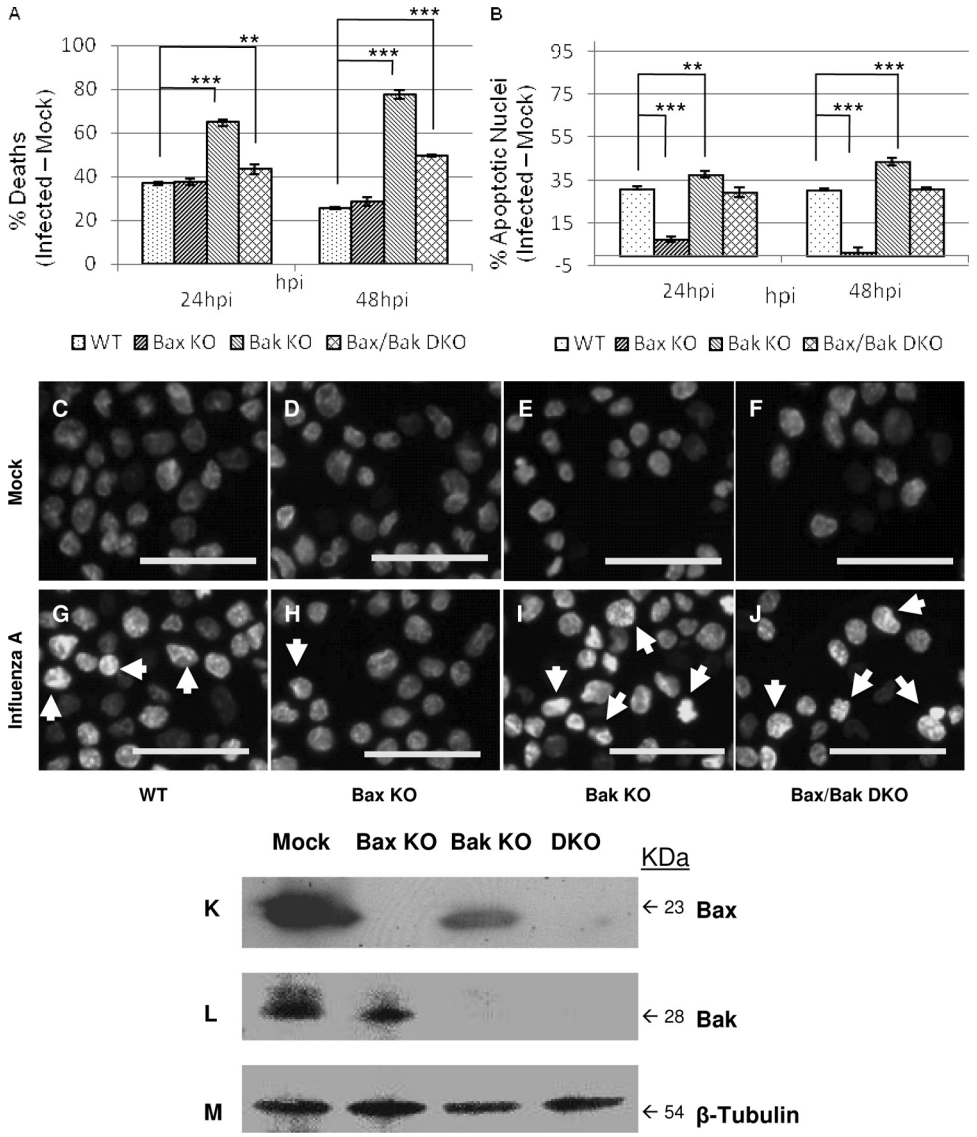

FIG. 2. Cell death and nuclear and mitochondrial alterations follow influenza A/WSN/33 virus infection in cells lacking Bax and/or Bak. (A) Total influenza virus-induced cell death was analyzed by trypan blue exclusion. While influenza A virus induces excessive cell death in Bak KO cells compared to the WT at 24 hpi and 48 hpi ($P < 0.0001$ and $P < 0.0002$, respectively), Bax KO cells do not differ from WT cells in the response to infection. Bax/Bak DKO cells show increased rates of death compared to the WT at 24 hpi and 48 hpi ($P = 0.03$ and $P = 0.000001$, respectively), indicating that Bax and Bak activities modulate death during infection. (B) Influenza A virus-induced nuclear condensation and fragmentation were analyzed by Hoechst staining. Bax KO cells exhibited a drastic reduction in nuclear alterations during influenza A virus infection compared to the WT at both 24 hpi and 48 hpi ($P < 0.00003$ and $P = 0.00015$, respectively). In contrast, Bak KO cells showed significant increases in influenza A virus-induced changes in nuclear morphology compared to the WT at 24 hpi and 48 hpi ($P = 0.04$ and $P = 0.0002$, respectively), while no significant difference was seen between Bax/Bak DKO and WT cells. These results suggest that influenza A virus may employ Bax as a means to trigger mitochondrial apoptosis during infection and that Bak antagonizes Bax in this situation. (C to J) Changes in nuclear morphology during influenza A virus infection were assessed by fluorescence microscopy at 48 hpi. Arrows mark nuclear condensation and fragmentation during influenza A virus infection, indicating apoptotic cell death. (C) WT mock; (D) WT plus influenza A virus; (E) Bax KO mock; (F) Bax KO plus influenza A virus; (G) Bak KO mock; (H) Bak KO plus influenza A virus; (I) Bax/Bak DKO mock; (J) Bax/Bak DKO plus influenza A virus. Bars, 50 μm. (K to M) KO of Bax and/or Bak was confirmed by Western blotting. (K and L) Bax is present only in WT and Bak KO cells (K), while Bak is present only in WT and Bax KO cells (L), confirming knockout in Bax KO, Bak KO, and Bax/Bak DKO cells. (M) β-Tubulin was used as a loading control.

shown in Fig. 2I, display almost no fragmented nuclei at 24 hpi. These results suggest that Bax activation is intimately involved in the induction of apoptosis by influenza A virus.

To confirm the identity of WT, Bax KO, Bak KO, and Bax/Bak DKO cells, total protein lysates were analyzed by Western blotting for the presence of Bax and Bak. Confirmation of Bax and/or Bak KO is shown in Fig. 2K and L, where Bax is present in both WT and Bak KO cells but not in Bax KO and Bax/Bak DKO cells, while Bak is present is WT and Bax KO cells but not in Bak KO and Bax/Bak DKO cells. To

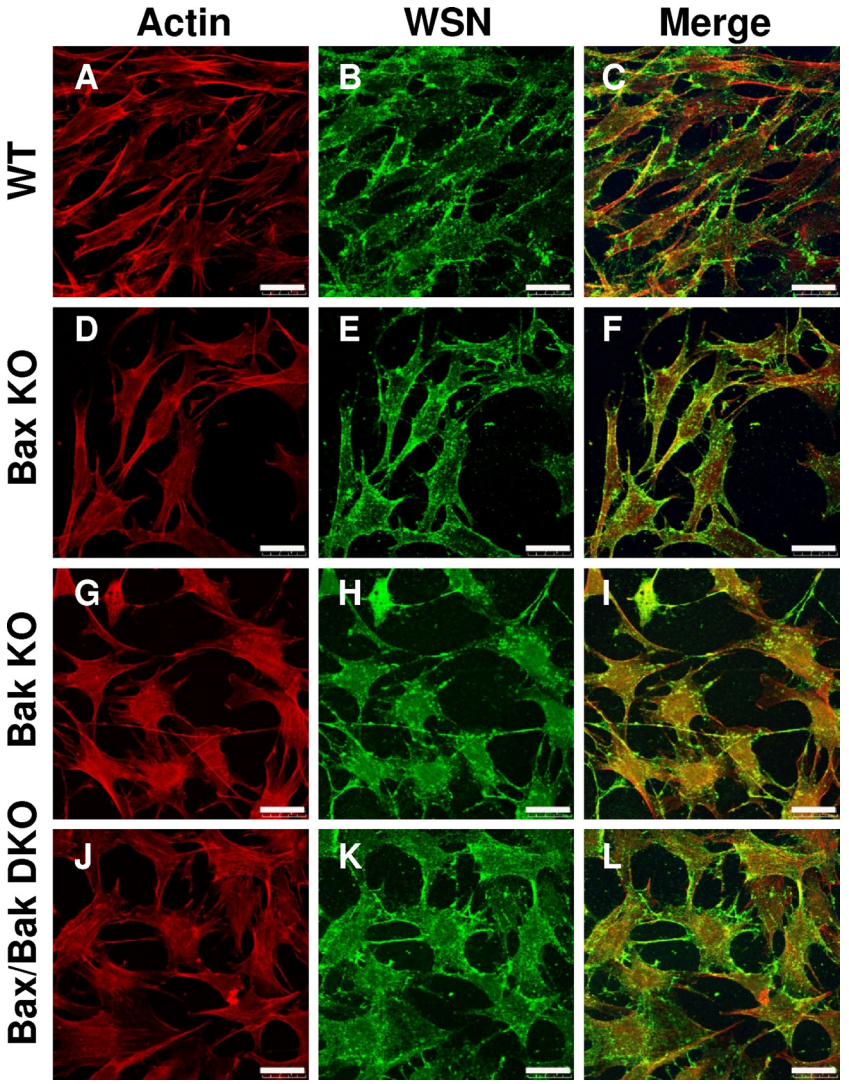

FIG. 3. Influenza A virus establishes infection and replicates in WT, Bax KO, Bak KO, and Bax/Bak DKO cells. Actin was stained by phalloidin-TRITC (A, D, G, and J). Immunocytochemical staining of influenza A virus-infected cells at 24 hpi with anti-WSN whole-virus primary antibody, followed by Alexa Fluor 488 staining (B, E, H, and K). Reveals cytoplasmic influenza A virus-induced vesicles containing mature virions in all infected cells regardless of Bax and/or Bak activity. (C, F, I, and L) Merge. Bars, 10 μm.

confirm infection of each cell type, cells were infected at and MOI of 5 and fixed at 24 hpi. Immunocytochemistry using anti-influenza A/WSN virus was performed with infected cells and observed by confocal microscopy. As shown in Fig. 3, by 24 hpi, virus-induced vesicles were present in all cell types, confirming the ability of influenza A virus to infect and replicate regardless of the presence of Bax or Bak.

The observed differences in death rates in Bax and/or Bak KO cells following infection may arise from differences in subsequent perturbations of apoptotic signaling. To further characterize the involvement of Bax and Bak in influenza A virus-induced apoptosis, we examined cytochrome *c* localization at 24 hpi by immunocytochemistry. As shown in Fig. 4A to D, cytochrome *c* is distributed in a punctate pattern consistent with mitochondrial localization, and there is minimal cytoplasmic localization of cytochrome *c* in mock-infected cells at 24 hpi. In influenza A virus-infected WT (Fig. 4E) and Bak KO (Fig. 4G) cells, strong cytoplasmic cytochrome *c* staining is evident at 24 hpi. This corresponds to the observed apoptotic death in these cells following infection. Bax KO (Fig. 4F) and Bax/Bak DKO (Fig. 4H) cells do not exhibit detectable cytoplasmic cytochrome *c* staining, indicating a block in cytochrome *c* release after infection in cells lacking Bax. We also looked for an activation of caspase-3 using an antibody specific to active caspase-3. As shown in Fig. 4I to L, caspase-3 is not activated by 48 hpi in mock-infected WT or KO cells, corresponding to the lack of death observed in these populations. However, in influenza A virus-infected WT (Fig. 4M), Bak KO (Fig. 4O), and Bax/Bak DKO (Fig. 4P) cells, strong staining indicative of activated caspase-3 was found, further demonstrating the induction of apoptosis in response to influenza A virus. On the other hand, in Bax KO MEFs (Fig. 4N), we found no such staining, indicating no activation of caspase-3 after infection in the absence of Bax.

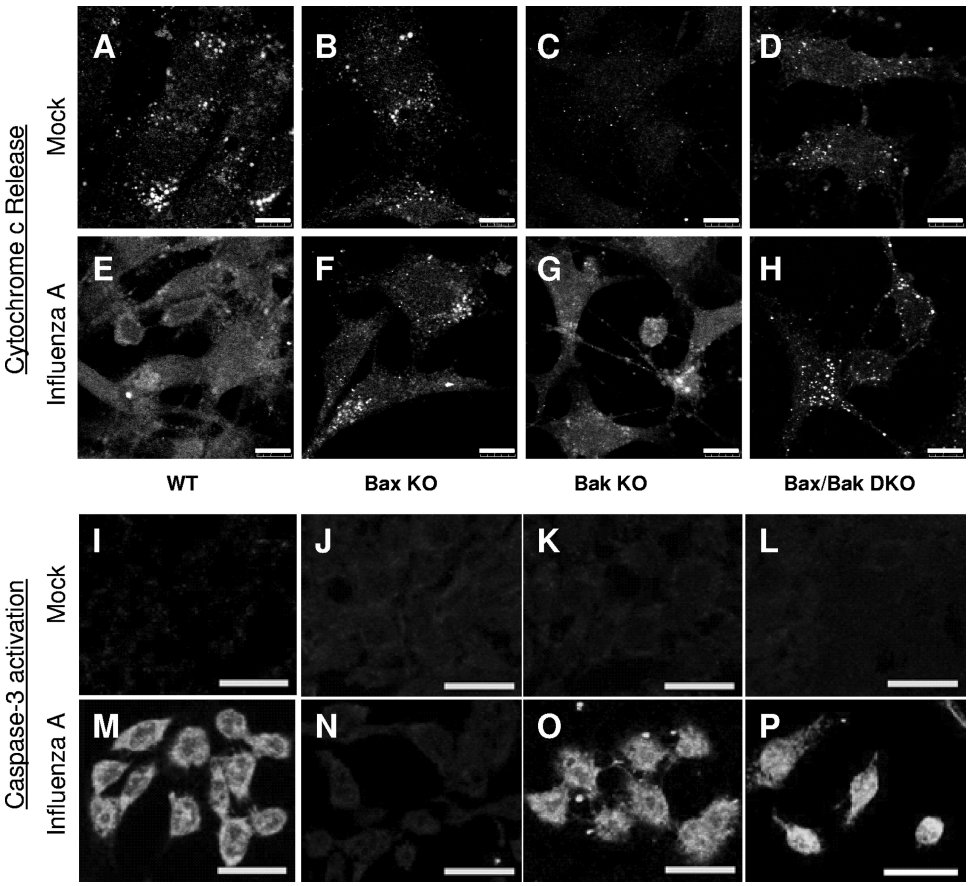

FIG. 4. Influenza A virus-induced cytochrome *c* release and subsequent caspase activation are dependent primarily on Bax signaling. (A to H) Immunocytochemical staining of cytochrome *c* release in cells lacking Bax and/or Bak following influenza A virus infection. (A to D) Cytochrome *c* staining reveals a punctate distribution consistent with mitochondrial localization in healthy, mock-infected cells of each type. (E and G) Following influenza A virus infection at 24 hpi, cytoplasmic cytochrome *c* is evident in WT (E) and Bak KO (G) cells. (F and H) Bax KO (F) and Bax/Bak DKO (H) cells show no appreciable cytochrome *c* release by 48 hpi and retain a punctate cytochrome *c* staining pattern. These results indicate that Bax is necessary for influenza A virus-induced cytochrome *c* release. (I to P) Immunocytochemical staining of active caspase-3 in cells lacking Bax and/or Bak following influenza A infection. (I to L) Staining for active caspase-3 yields no signal in healthy, mock-infected cells. (M, O, and P) Following influenza A virus infection at 48 hpi, widespread caspase-3 activation is evident in WT (M), Bak KO (O), and Bax/Bak DKO (P) cells. (N) Bax KO cells do not show appreciable caspase-3 activation following influenza A virus infection, indicating that Bax, in the presence of Bak, is necessary for caspase-3 activation by influenza A virus. The activation of caspase-3 in Bax/Bak DKO cells indicates that there is an alternative pathway to caspase activation during influenza A virus infection in the absence of both Bax and Bak.

Executioner caspase activation was confirmed by Western blotting of extracted whole-protein lysate from mock- and influenza A virus-infected MEFs of WT and KO cells at 24 hpi. Antibodies specific to the activated forms of caspase-3 and caspase-7 were used to confirm the activation of caspase. Activated caspase-3, shown in Fig. 5A, was observed in both WT and Bak KO cells following infection. Caspase-3 activation was also apparent in Bax/Bak DKO cells albeit at reduced levels compared to those of the WT. Likewise, activated caspase-7, shown in Fig. 5B, was seen only in influenza A virus-infected WT and Bak KO cells and was absent in Bax KO cells following infection. In contrast to the caspase-3 activation shown in Bax/Bak DKO cells following infection, caspase-7 activity in these cells was only slightly apparent at 24 hpi. To confirm that we had a robust level of infection in all the cells, an antibody specific to influenza A virus NP was used to detect the production of viral protein. Figure 5D shows that high levels of influenza A virus NP are present in infected WT cells and each KO cell condition, confirming that each cell type is permissive to viral infection. Consistent with the viral RNA levels (discussed below) (Fig. 5C), all three KO conditions showed stronger NP staining than the WT. Bcl-2 expression was not affected by influenza A virus infection in any of these cells (Fig. 5C). β-Tubulin was used as a loading control (Fig. 5E). These results suggest that the observed differences between cell types arise downstream of Bcl-2 activity and not from indirect effects upstream of Bax and Bak.

We next quantified the combined activities of caspase-3 and caspase-7 following infection by assessing the cleavage of a fluorogenic caspase-3/7 substrate, rhodamine 110, bis(*N*-carbobenzyloxy-L-aspartyl-L-glutamyl-L-valyl-L-aspartic acid amide [Z-DEVD-R110]), as described in Materials and Methods. A substantial increase in fluorescence was seen following infection in WT, Bak KO, and Bax/Bak DKO cells, closely corresponding to the observed patterns of apoptotic nuclei in these cells in

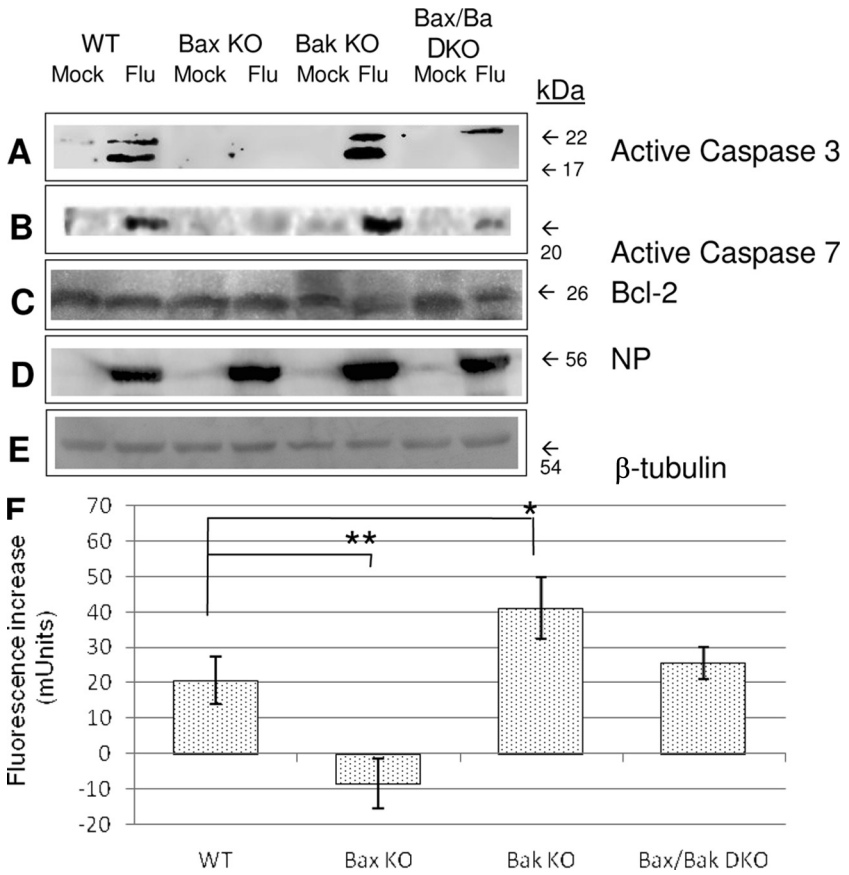

FIG. 5. Executioner caspase activation does not occur after infection of Bax KO cells. (A to E) Western blotting for executioner caspase activation in influenza A virus-infected cells lacking Bax and/or Bak. Immunoblotting was performed with antibodies specific for active caspase-3 (A), cleaved caspase-7 (B), Bcl-2 (C), influenza A virus NP (D), and β-tubulin (E), which was used as a loading control. An activation of caspase-3 and caspase-7 was not seen in Bax KO MEFs and was impaired in Bax/Bak DKO cells, whereas caspase activation was evident in WT and Bak KO cells that constitutively expressed Bax. Bcl-2 expression was constant across all cell types in both mock- and influenza A virus-infected cells. (F) Executioner caspase activity (caspase-3 and caspase-7) was assessed using and Apo-One caspase activity kit, and cleavage of fluorogenic substrate was assessed at 495 nm by use of a fluorescence microplate reader (Bio-Tek). Data are expressed as arbitrary units (milliunits [mUnits]), (fluorescence from influenza A virus-infected cells) − (fluorescence from mock-infected cells), in individual wells. The rate of activated executioner caspase substrate cleavage was high in Bak KO cells compared to the WT ($P = 0.03$), but the substrate was largely uncleaved in Bax KO cells following infection ($P = 0.007$), indicating that Bax in the presence of Bak is required for executioner caspase activation in response to influenza A virus.

response to the virus (Fig. 5F). Bax KO cells demonstrated no appreciable increase in fluorescence levels following influenza A virus infection, providing further evidence that caspase-3 and caspase-7 are not activated under this condition.

Overall, we demonstrate that mitochondrion-mediated apoptotic signaling through Bax is essential for an apoptotic response to influenza A virus. Cells lacking Bax still die in response to infection although not by apoptosis.

Bax KO forces influenza A virus-infected cells into an increased autophagic state. Although influenza A virus-induced signaling for apoptosis is inhibited in Bax KO cells, the number of cells that die in response to infection is approximately equal to that of the WT, suggesting that when Bax-mediated apoptosis is restricted during infection, an alternative death pathway is triggered. We have found that in influenza A virus-infected MDCK cells, a pharmacological blockade of caspase activation yields an increase in rates of autophagosome production and cell death (Shirazian et al., unpublished). Therefore, we evaluated the role of autophagy or lysosomal activity during influenza A virus-induced death of cells lacking Bax or Bak. To this end, we determined the activity of lysosomal acid phosphatase as an indicator of lysosomal activity. As shown in Fig. 6A, influenza A virus-infected WT cells showed a decrease in levels of acid phosphatase activity compared to that of mock-infected cells, with a smaller decrease displayed by Bak KO cells after infection. In contrast, a marked increase in acid phosphatase activity levels was seen in Bax KO cells after infection, with Bax/Bak DKO cells exhibiting a lower level of increase in response to influenza A virus.

Using LysoTracker staining and FACS analysis, we also found an increase in lysosomal volume in WT, Bak KO, and Bax/Bak DKO cells, with a slight decrease in the lysosomal volume of Bax KO cells after infection (Fig. 6B). Bax has been shown to induce lysosomal permeabilization under conditions of cellular stress (2), and pharmacological and genetic inhibition of Bax has been shown to inhibit lysosomal permeabilization as well as mitochondrion-induced apoptosis (2, 9, 13). We speculate that the influenza A virus-induced decrease in lyso-

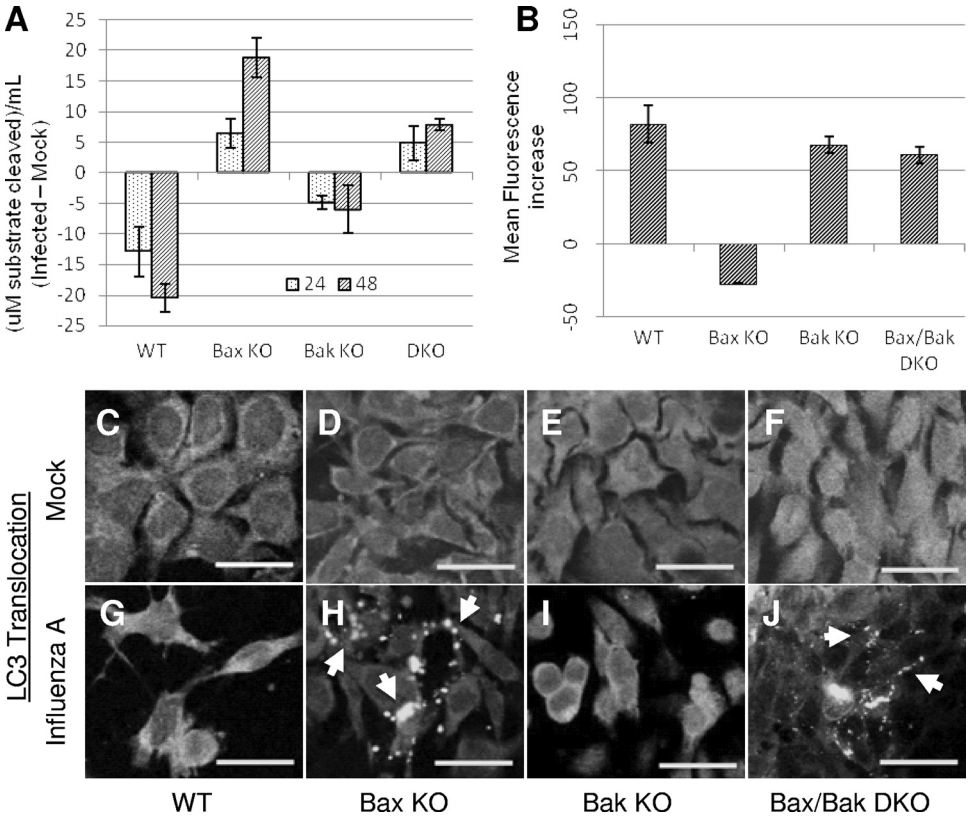

FIG. 6. Influenza A virus induces autophagy-like death in the absence of Bax. (A) Lysosomal acid phosphatase activity in influenza A virus-infected cells was assessed by measuring the release of *p*-nitrophenol from *p*-nitrophenylphosphate substrate. In cells constitutively expressing Bax, acid phosphatase activity decreases following infection, as these cells follow an apoptotic path to death. In cells lacking Bax, acid phosphatase activity increased, indicating an increase in lysosomal activity, a common marker for autophagic death. One unit equals 1 μmol of 4-nitrophenylphosphate per minute under the experimental conditions. (B) Cells were infected for 48 hpi and stained with Lysotracker Red DND-99 for 30 min prior to collection and immediate analysis by FACS. In WT, Bak KO, and Bax/Bak DKO cells, influenza A virus infection results in an increase in lysosomal volume by 48 hpi. In Bax KO cells, a slight decrease in lysosomal volume was observed by 48 hpi. (C to J) Cells were transfected with a construct expressing LC3-GFP prior to infection and observed by confocal microscopy for LC3 expression and translocation following infection. (C to F) The diffuse LC3-GFP expression pattern in mock-infected cells indicates a cytoplasmic, inactive distribution of LC3 in each cell type. (G and I) In cells constitutively expressing Bax, LC3-GFP expression remains diffuse following infection, indicating a lack of LC3 activation as these cells undergo apoptosis. (H and J) In cells lacking Bax (Bax KO and Bax/Bak DKO cells), LC3-GFP staining shifts to a punctate pattern, indicating LC3 activation and translocation to autophagosomes, a process that occurs solely during autophagy. Bars, 25 μm.

somal activity (as demonstrated by acid phosphatase activity) in WT and Bak KO cells reflects a Bax-dependent leakiness of the lysosomes (evident by the increase in lysosomal volume after infection), resulting in a loss of acidity and, hence, a loss of lysosomal enzyme activity. In Bax KO cells, there is an increase in levels of acid phosphatase activity together with a slight decrease in lysosomal volume, which is likely due to a lack of lysosomal permeabilization after infection with influenza A virus in these cells. Together, these data suggest an increase in lysosomal activity following infection in cells lacking Bax. However, Bax/Bak DKO cells also show an increase in acid phosphatase activity after infection but without the corresponding lack of lysosomal swelling seen in Bax KO cells, suggesting the existence of a parallel pathway to lysosomal permeabilization following infection when both Bax and Bak are missing.

As stated above, blocking caspase activity increases the formation of autophagosomes following infection (Shirazian et al., unpublished). We therefore assessed the autophagic response to influenza A virus in cells lacking Bax, which do not activate caspase-3, by examining LC3 localization during infection (Fig. 5). Inactive LC3 is cytoplasmic, resulting in a diffuse staining pattern unless cleaved and activated during autophagy. LC3 cleavage results in its translocation to autophagosomal membranes, where it accumulates and appears as a brightly punctate staining pattern. To examine LC3 localization, we expressed a C1-LC3-GFP construct in the different cell types, infected the cells, and assessed the expression and localization of the construct. As shown in Fig. 6C to F, in WT and all KO cells, mock-infected cells displayed the diffuse pattern of expression of LC3-GFP consistent with an inactive, cytoplasmic LC3-GFP distribution. Following infection, cells constitutively expressing Bax (WT and Bak KO) continued to display the diffuse LC3-GFP expression pattern at 24 hpi (Fig. 6G and I, respectively). This result indicates that autophagosome formation is not triggered following infection of cells expressing functional Bax and is consistent with an apoptotic response. However, in cells lacking functional Bax (Bax KO and Bax/Bak DKO cells), LC3-GFP shifts to a punctate pattern of distribution by 24 hpi (Fig. 6H and J, respectively), consis-

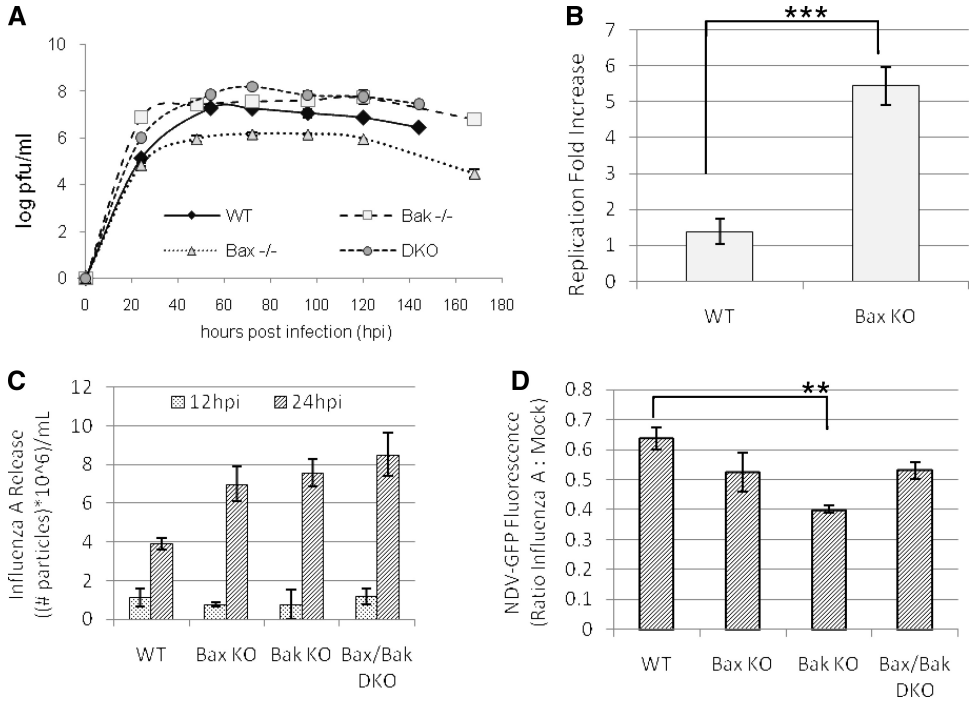

FIG. 7. Influenza A virus replication is dependent upon opposite virus-induced effects on Bax and Bak activity that are unlikely to be interferon related. (A) Influenza A virus replication was analyzed by plaque assay. Virus replication is severely attenuated in Bax KO cells, resulting in a 2-log decrease in PFU/ml compared to the WT. Bak KO cells allow a maximum replication similar to that of the WT, while Bax/Bak DKO cells show a slight elevation of infectious titers during infection. These results indicate that Bax is proviral during infection, while Bak is dispensable for replication. (B) Bax was transiently expressed in all cell types by Lipofectamine 2000 transfection of a C2-Bax-GFP construct prior to infection, and supernatant samples were collected for plaque assay at 48 hpi. Baseline virus replication in each cell type was evaluated using empty C2-GFP plasmid transfection. Bax reconstitution in Bax KO cells resulted in a fivefold increase in infectious titers compared to the control ($P = 0.0007$). A minimal effect on the virus titer was seen after Bax overexpression by transient transfection in WT cells compared to empty plasmid controls. (C) Influenza A virus replication was assessed by reverse transcription-PCR. Serial dilutions of stock virus at known concentrations were also analyzed to generate a standard curve to which experimental samples were compared, thus calculating the approximate number of influenza A virus particles/ml in each sample. By 24 hpi, Bax KO, Bak KO, and Bax/Bak DKO cells all showed significantly higher levels of influenza A virus RNA released into the cell culture supernatant than did WT cells. (D) Interferon activity was assessed by infecting mock- and influenza A virus-infected cells with interferon-sensitive, GFP-linked NDV and quantifying the mean GFP expression levels of 10,000 events per condition by FACS analysis. Each assay was run in triplicate, and data are expressed as the ratio of the numbers of influenza A virus-infected to mock-infected cells per cell type. After influenza A virus infection, Bak KO cells exhibited a slight decrease in ratio compared to the WT, representing a 30% increase in interferon activity ($P = 0.002$). Bax KO and Bax/Bak DKO cells both showed similar fluorescence changes compared to the WT after infection. Due the high degree of similarity between cell types, these results suggest that the interferon response in infected cells is modulated by viral replication in the presence of Bak and is only slightly modified by Bax activity during influenza A virus infection. As an elevated interferon response typically leads to a reduced virus replication capacity, these results also suggest that it is unlikely that the observed trends in infectious virus titer are due to virus-induced interferon signaling.

tent with LC3 translocation to autophagosomal membranes. These results indicate that when Bax-mediated caspase activation is blocked during influenza A virus infection, an alternative cell death path that employs an increase in the autophagic state is in play, which leads to cell death by this alternative route.

Bax expression is required for efficient replication of influenza A virus, while Bak suppresses replication. The observations reported here demonstrate that influenza A virus-induced apoptosis is driven primarily by the intrinsic pathway, most likely derived from Bax translocation and the subsequent cytochrome *c* release from mitochondria. The downregulation of Bak expression following infection indicates that Bak is suppressed by the virus, suggesting an adaptation of the virus to suppress an antivirus function. To evaluate this possibility, we examined the effect of the elimination of Bax and/or Bak on the virus replication cycle as determined by the titers of infectious virus. Cell supernatant samples from infected cells were collected every 24 h until 144 hpi. These samples were used to infect monolayers of MDCK cells for analysis of viral replication by plaque assay. The virus titer reached a maximum of 10^7 PFU/ml in WT cells at 48 hpi and decreased slightly thereafter (Fig. 7A). However, Bak KO cells exhibited a much faster production of virus and surpassed the WT maximum titer by 24 hpi. The titer in Bak KO cells then reached a maximum titer similar to that of the WT by 72 hpi of just over 10^7 PFU/ml, and these cells maintained this titer to 144 hpi ($P < 0.000002$ at 24 hpi; $P = 0.08$ at 48 hpi; $P = 0.14$ at 72 hpi; $P = 0.016$ at 96 hpi; $P = 0.09$ at 120 hpi; $P = 0.01$ at 144 hpi) (Fig. 7A). On the other hand, Bax/Bak DKO cells reached a maximum titer of 10^8 PFU/ml at 24 hpi, which is 10-fold higher than that of the WT, and the titer then declined slightly until 144 hpi ($P = 0.0004$ at 24 hpi; $P = 0.002$ at 48 hpi; $P = 0.14$ at 72 hpi; $P = 0.016$ at 96 hpi; $P = 0.09$ at 120 hpi; $P = 0.01$ at 144 hpi) (Fig.

7A). In contrast, the production of infectious virus as indicated by plaque assay is substantially inhibited in Bax KO cells, reaching a maximal titer of only 10^5 PFU/ml by 48 hpi, much lower than that of the WT ($P = 0.012$ at 24 hpi; $P = 0.003$ at 48 hpi; $P = 0.0004$ at 72 hpi; $P = 0.01$ at 96 hpi; $P = 0.00001$ at 120 hpi; $P = 0.0005$ at 144 hpi) (Fig. 7A). By 48 to 60 hpi, virtually all of the cells were dead and viral replication had ceased, with viral replication in Bax KO cells never having reached the level seen in the WT; the results beyond 48 hpi represent survival of virus. These results suggest that the intrinsic signaling of apoptosis through Bax is an integral step in the influenza A virus replication cycle and that Bak is antiviral during the early stages of infection.

To confirm the involvement of Bax in the production of influenza A virus, we determined if Bax supplementation in Bax KO cells would rescue the Bax KO cells' deficiency in virus production. We expressed a plasmid C2-Bax-GFP construct in WT and Bax KO cells. Following influenza A virus infection for 48 hpi, the supernatant was collected for plaque assay. Empty C2-GFP plasmid was used as the control for each cell type. Under all conditions, plasmid expression was confirmed by microscopic examination of GFP expression (data not shown). As shown in Fig. 7B, the addition of Bax to Bax-containing WT cells had almost no impact on viral titer, but the replacement of Bax in Bax KO cells increased the viral titer fivefold ($P = 0.0007$), approaching normal titers. Therefore, we conclude that Bax-mediated signaling plays an integral role in influenza A virus replication.

The difference in virus titers among KO constructs may be derived from differences in viral genomic replication, assembly, or maturation. If these differences are due to genomic replication, fewer virions (and, therefore, less viral RNA) will be released from Bax KO cells than from WT cells, resulting in a lower plaque assay titer. However, if these differences are due to the assembly or maturation of progeny virions, Bax KO cells may release numbers of virions similar to those of WT cells but will produce fewer infectious progeny. Therefore, even if Bax KO and WT cells released similar amounts of viral RNA (viral particles), a plaque assay will show lower viral titers from Bax KO cells. To determine whether the differences in viral replication between cell types is due to differences in overall viral release or in virion infectivity, we quantified the amount of viral RNA released after infection. Viral RNA was extracted from the supernatant of infected cells at 24 hpi and subjected to reverse transcription-PCR using primers for influenza A virus HA. The amounts of RNA detected in all three KO cell types (Bax KO, Bak KO, and Bax/Bak DKO cells) remained similar at approximately double the amount released from infected WT cells (Fig. 7C). It appears that although each KO condition allows an increase in the level of production of viral RNA similar to that of the WT, this increase is not coupled with an associated increase in viral infectivity. Thus, the differences in the clonigenicity of the virus cannot be explained entirely by differential viral genomic expression and may be derived in part from defects in virus assembly or maturation. We therefore searched for these defects.

Decrease in titer by Bax KO is not directly related to interferon. Interferon inhibits the replication of many viruses through the use of several mechanisms (15, 22, 25, 30, 39). Although the influenza A virus NS1 protein is a potent inhibitor of interferon (1, 4, 10, 15, 39), the differential induction of interferon in Bax and/or Bak KO cells compared to that of the WT could also account for the differences in virus replication observed between cell types. We therefore assessed interferon activity in infected WT, Bax KO, Bak KO, and Bax/Bak DKO cells using GFP-tagged NDV, which is highly sensitive to interferon. Interferon activity after infection of cells with influenza A virus can be indirectly quantified by secondary infection with NDV-GFP, followed by the measurement of GFP fluorescence by FACS (24, 25, 30). As shown in Fig. 7D, levels of interferon activity are elevated (NDV-GFP levels are decreased) by influenza A virus infection under WT and all KO conditions. Infected Bax KO cells showed a level of NDV-GFP replication similar to that of the WT, whereas infected Bak KO cells showed a significant decrease in levels of NDV-GFP replication, representing an approximately 30% increase in interferon activity compared to those observed for both WT ($P = 0.002$) and Bax KO ($P = 0.037$) cells. The Bax/Bak DKO cells show a response similar to those of Bax and WT cells. These results suggest that Bak potentiates the interferon response in influenza A virus-infected cells and are consistent with the effects of Bak KO on virus replication and a model in which Bak suppresses the replication of influenza A virus. As the interferon response to infection observed in Bax KO cells is very similar to those of WT and Bax/Bak DKO cells, these data also indicate that excess interferon signaling is not responsible for the observed decline in the titer of infectious virus in Bax KO cells.

Absence of Bax leads to inappropriate nuclear retention of influenza A virus NP. The lack of caspase-3 activity following infection with influenza A virus results in influenza A virus NP retention within the nucleus (26, 41), sequestering viral genomic segments within the nucleus away from the cytoplasmic viral assembly sites. As influenza A virus NP acts as a shuttle for viral genomic segments from the nucleus to cytoplasmic assembly centers, its location during the virus replication cycle markedly influences virus titers. A significant retention of influenza virus NP as a result of Bax KO cells within the nucleus would impair the proper assembly of progeny virions, thus reducing their infectivity. Similarly, lysosomal sequestration of viral segments in these cells during an autophagic response may also lead to improper viral assembly. To determine if the lack of Bax and/or Bak signaling plays a role in the nuclear export of influenza A virus NP or if the autophagic response seen in cells lacking Bax causes the sequestration of virus segments in autophagosomes, the localization of influenza A virus NP was determined at 24 hpi by using an antibody specific to influenza A virus NP coupled with organelle identification by DAPI (nucleus) and LysoTracker Red (lysosomes) under WT and all KO conditions. As shown in Fig. 8D, H, L, and P, at 24 hpi, influenza A virus NP does not colocalize with lysosomes in either WT or KO cells. This suggests that that the reduced rate of virus replication in Bax KO cells does not derive from the lysosomal sequestration of viral genomic segments or viral progeny. As shown in Fig. 8C, very small vesicles containing influenza A virus NP are apparent in WT cells throughout the cytoplasm and at the cell membrane, with no nuclear NP staining being evident at 24 hpi. Influenza A virus-containing vesicles are similarly small in Bak KO cells, with viral NP localizing near the cell membrane (Fig. 8L),

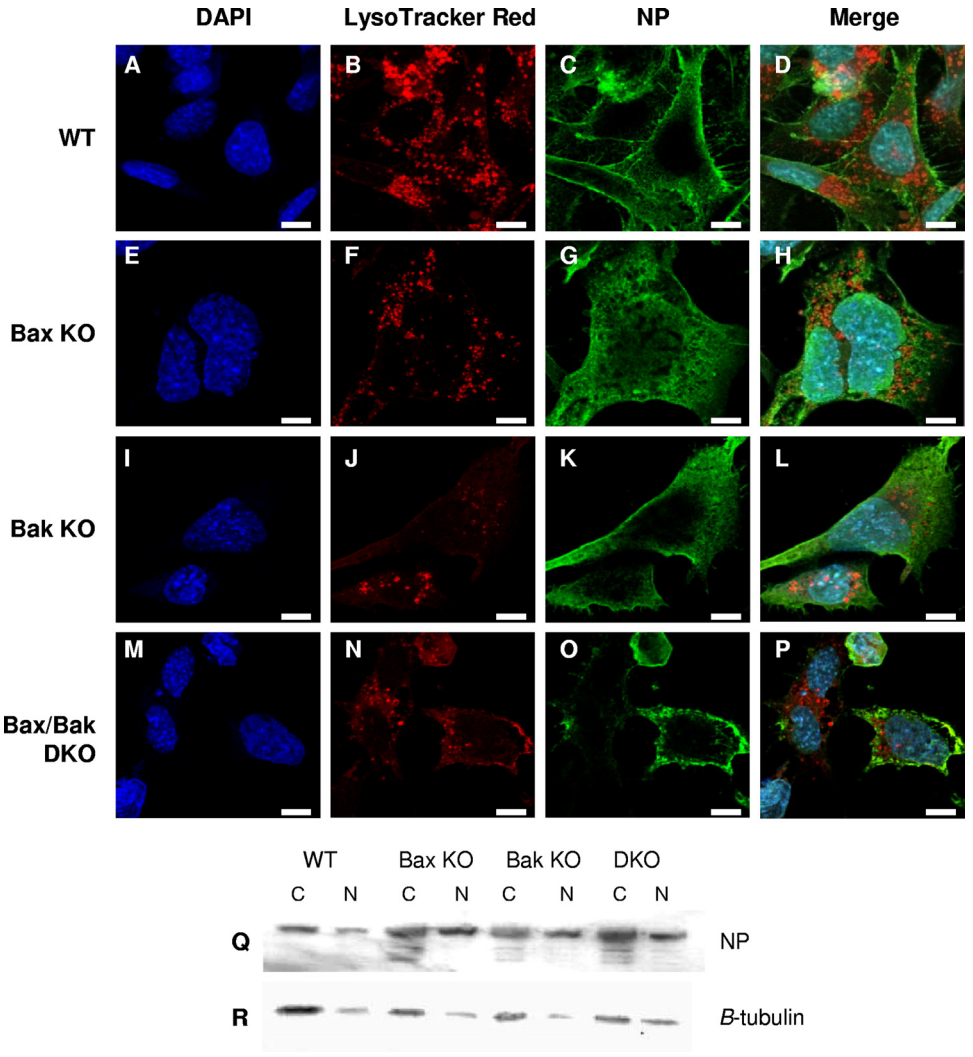

FIG. 8. Influenza A virus NP exhibits increased nuclear retention in Bax KO cells. Nuclear retention of NP due to a lack of caspase activity has been linked to decreased titers of virus. DAPI staining was used for nuclear localization (A, E, I, and M), lysosomes were stained with LysoTracker Red DND-99 (B, F, J, and N), and influenza A virus NP localization was determined using an NP-specific antibody (C, G, K, and O). Images were taken using a confocal microscope. (D, H, L, and P) Merge. Lysosomal localization of influenza A virus NP was not observed in WT cells or any of the KO cells. NP showed near-complete cytoplasmic localization in WT cells (D) and Bax/Bak DKO cells (P). A slight nuclear retention of NP was observed in Bak KO cells (L), while in Bax KO cells (H), a nuclear retention of influenza A virus NP is obvious in all infected cells. Bars, 10 μm. (Q) Nuclear retention of NP in infected Bax KO and, to a lesser extent, Bak KO cells was confirmed by Western blotting of cytoplasmic (C) and nuclear (N) fractions of infected cells. (R) β-Tubulin was used to ensure efficient fractionation.

suggesting an efficient endocytic release of viral progeny despite the slight nuclear NP staining evident in roughly 50% of these cells. Influenza A virus NP localizes in the cytoplasm and near the cell surface, with little apparent nuclear NP staining evident in Bax/Bak DKO cells (Fig. 8P). However, in Bax KO cells (Fig. 8H), nuclear NP staining is evident in nearly all infected cells. To confirm that excessive nuclear retention of influenza A virus NP occurs in Bax KO cells but not in WT, Bak KO, and Bax/Bak DKO cells, nuclear and cytoplasmic proteins of infected cells were obtained as described in Materials and Methods. As shown in Fig. 8Q, strong staining for influenza A virus NP is located in the cytoplasmic fraction of all infected cells. In WT cells, very little NP staining was seen in the nuclear fraction. However, there was strong NP staining in Bax KO cells, confirming NP enrichment in the nuclear fraction of these cells. Bak KO and Bax/Bak DKO cells also showed some NP enrichment after infection although not as severe as that for infected Bax KO cells. While these results suggest that both Bax and Bak have an effect on viral NP trafficking between the nucleus and cytoplasm, they indicate that the abolition of Bax-mediated apoptosis, with concurrent Bak activity, yields a particularly effective restriction of NP export from the nucleus to cytoplasmic viral assembly centers.

DISCUSSION

Several groups have linked an apoptotic response in influenza A virus-infected cells to the efficiency of virus replication. While purposeful cell killing may seem to be counterintuitive

for maximizing virus replication, an activation of apoptosis is required by influenza A virus for proper viral RNP complex release from the nucleus to cytoplasmic viral assembly centers (41) as well as for proper viral HA processing prior to progeny release (29). The specific importance of mitochondrion-mediated caspase activation in this event has not been clearly studied. Here we report that influenza A virus manipulates both Bax- and Bak-mediated apoptosis, affecting both the cell death phenotype and efficiency of virus replication and propagation.

Bcl-2 suppresses apoptosis by sequestering Bax and Bak (7), and Bcl-2 overexpression in MDCK cells causes a reduction in both apoptosis and virus replication (29). MDCK cells, which lack functional Bcl-2 (12, 17), permit influenza A virus infection. We will present evidence of high-virus-titer generation as apoptosis proceeds with cytochrome *c* release and the activation of the caspase cascade elsewhere (data not shown). Therefore, the activation of Bax and/or Bak, which Bcl-2 opposes, may provide an integral step in the formation of viral progeny. Consistent with these results, we find that while Bak expression is severely downregulated in MDCK cells following infection, Bax translocation from a diffuse cytoplasmic distribution to a punctate pattern indicates Bax activation in response to the virus despite a reduction in expression levels following infection. These results suggest a selection pressure for influenza A virus favoring Bax activity with a concurrent disruption of Bak signaling during infection.

To understand the opposing effects of influenza A virus on Bax and Bak activity, we used MEF cells that lack Bax and/or Bak but express functional Bcl-2. In cells lacking Bak (which is severely downregulated during infection), the rates of both apoptosis (demonstrated by nuclear morphology, trypan blue exclusion, cytochrome *c* release, and the activation of caspases) and viral replication are increased compared to those of the WT. Thus, selection pressure for the virus favoring mitochondrion-mediated apoptosis activation may explain the observed reduction in Bak expression levels following infection in MDCK cells.

In contrast to Bak, Bax activation is essential for influenza A virus-induced caspase activation, and Bax is required for efficient virus replication. This is demonstrated by the near-complete lack of apoptosis markers present in Bax KO cells after infection, including nuclear condensation/fragmentation, cytochrome *c* release, and the activation of executioner caspase. In the absence of Bax activity, the virus titer is 1% of that seen in the WT. This effect is ameliorated by ectopic Bax expression, which increases virus replication in Bax KO cells. Overall, though, the rate of cell death in response to the virus is not reduced compared to that of the WT, indicating the involvement of an alternative death pathway. The general inhibition of caspases by the pancaspase inhibitor ZVAD-fmk (carbobenzoxy-valyl-alanyl-aspartyl-[*o*-methyl]-fluoromethylketone) shifts infected MDCK cells from apoptosis to autophagy and slightly decreases the overall rate of cell death (Shirazian et al., unpublished). Consistent with these results, Bax KO leads to the death of infected cells, with an increase in the levels of lysosomal activity and autophagy, as demonstrated by a dramatic increase in lysosomal acid phosphatase enzyme activity and LC3 translocation.

Interestingly, both cell death in response to infection and maximum virus titers are potentiated in Bax/Bak DKO cells compared to the WT. Similar numbers of apoptotic nuclei are found by comparing Bax/Bak DKO to WT cells following infection, indicating the involvement of an alternative, nonmitochondrial apoptosis pathway when Bax and Bak are absent. Alternative mechanisms may include the activation of the extrinsic apoptosis pathway, lysosomal protease, or calpain (32). The TRAIL and Fas/FasL death receptor systems can activate executioner caspases through capase-8 (36, 37). The caspase cascade may also be activated through lysosomal proteases, and there can be significant cross talk between caspase and calpain (27, 31). Although influenza A virus can trigger many different routes to caspase activation, the rate at which each one proceeds following infection is likely to vary. Our data argue that Bax-mediated apoptosis is a primary pathway by which influenza A virus induces cell death. More Bax/Bak DKO cells die than do WT cells following infection, without a corresponding rise in numbers of apoptotic nuclei, indicating that an alternative, nonapoptotic death pathway is initiated in a subset of the population. Consistent with this model, both apoptotic and autophagic cells are found in infected Bax/Bak DKO cells. Also, the dramatic increase in the rate of cell death observed for infected Bak KO cells is attenuated for Bax/Bak DKO cells, indicating that the interplay between Bax and Bak is an important component of influenza A virus-induced, mitochondrion-initiated death.

The decline in virus titers in Bax KO cells is not accompanied by a decrease in levels of viral RNA released from infected cells. This indicates that the reduction of viral titers seen in Bak KO cells results from a block in viral maturation or processing rather than a direct effect on viral genomic replication. Autophagosomal sequestration of viral genomic segments is an unlikely explanation for titer reductions in the absence of Bax, since influenza virus NP is not found in lysosomes. However, while WT cells show no nuclear NP staining at 24 hpi, nearly all Bax KO cells demonstrate a marked nuclear retention of viral NP along with a concurrent cytoplasmic localization. Western blotting of both the nuclear and the cytoplasmic fractions of infected cells also demonstrates nuclear NP enrichment in Bax KO cells compared to the WT. These results suggest that although many viral RNP complexes reach cytoplasmic assembly centers following infection in Bax KO cells, a large subset of viral RNP complexes and, therefore, their associated viral genomic segments are retained in the nucleus. This would lead directly to improper viral assembly and is a possible explanation for the observed reduction in overall viral infectivity. The data support a model in which infecting influenza A virus encounters proviral Bax and antiviral Bak. Bak may inhibit the Bax-mediated initiation of cell death. It is likely that viral PB1-F2, which is similar in structure and function to Bax (7), is involved in the interaction. We are currently exploring this possibility.

In summary, we identify Bax-mediated apoptosis as a driving force behind influenza A virus-induced cell death. In the presence of Bax, infected cells undergo apoptosis, and virus replication succeeds, while Bak suppresses apoptosis and viral replication The biochemical interactions and dynamics between Bax-mediated cytochrome *c* release and various other death pathways that drive this decision remain to be elucidated. However, it is clear that the success of viral

replication, i.e., the titer achieved during infection, depends on the interplay of Bax and Bak and how and when they affect cell death.

ACKNOWLEDGMENTS

We thank Adolfo Garcia-Sastre of Mt. Sinai Medical School for providing the GFP-tagged Newcastle disease virus and influenza A virus NP antibody and intellectual advice. We thank Guido Kroemer for providing a number of plasmids used in our experiments and the late Stanley Korsemeyer for providing the different KO cells used in this paper. We give special thanks to Michelle Sahli and Aleksandra Wudzinska for providing technical and editorial support. We also thank Areti Tsiola of the Queens College Core Facility for Imaging, Molecular and Cellular Biology, for technical expertise. We especially thank Richard Lockshin for a critical review of the manuscript prior to its submission.

This work was supported in part by funding from the NIH (MARC-USTAR), grant 2T34GM070387-03, to Zahra F. Zakeri and by a PSCCUNY award to Zahra F. Zakeri.

REFERENCES

1. **Bergmann, M., A. Garcia-Sastre, E. Carnero, H. Pehamberger, K. Wolff, P. Palese, and T. Muster.** 2000. Influenza virus NS1 protein counteracts PKR-mediated inhibition of replication. J. Virol. **74:**6203–6206.
2. **Boya, P., K. Andreau, D. Poncet, N. Zamzami, J.-L. Perfettini, D. Metivier, D. M. Ojcius, M. Jaattela, and G. Kroemer.** 2003. Lysosomal membrane permeabilization induces cell death in a mitochondrion-dependent fashion. J. Exp. Med. **197:**1323–1334.
3. **Brydon, E. W. A., S. J. Morris, and C. Sweet.** 2005. Role of apoptosis and cytokines in influenza virus morbidity. FEMS Microbiol. Rev. **29:**837–850.
4. **Brydon, E. W. A., H. Smith, and C. Sweet.** 2003. Influenza A virus-induced apoptosis in bronchiolar epithelial (NCI-H292) cells limits pro-inflammatory cytokine release. Soc. Gen. Microbiol. **84:**2389–2400.
5. **Chen, W., P. A. Calvo, and D. Malide.** 2001. A novel influenza A virus mitochondrial protein that induces cell death. Nat. Med. **7:**1306–1312.
6. **Cheng, E. H.-Y., T. V. Sheiko, J. K. Fisher, W. J. Craigen, and S. J. Korsemeyer.** 2003. VDAC2 inhibits Bak activation and mitochondrial apoptosis. Science **301:**513–517.
7. **Chipuk, J. E., and D. R. Green.** 2008. How do BCL-2 proteins induce mitochondrial outer membrane permeabilization? Trends Cell Biol. **18:**157–164.
8. **Feldstein, A. E., N. W. Wernenburg, Z. Li, S. F. Bronk, and G. J. Gores.** 2006. Bax inhibition protects against free fatty acid-induced lysosomal permeabilization. Am. J. Physiol. Gastrointest. Liver Physiol. **290:**G1399–G1346.
9. **Fink, S. L., and B. T. Cookson.** 2005. Apoptosis, pyroptosis, and necrosis: mechanistic description of dead and dying eukaryotic cells. Infect. Immun. **73:**1907–1916.
10. **Garcia-Sastre, A., A. Egorov, D. Matassov, S. Brandt, D. E. Levy, J. E. Durbin, P. Palese, and T. Muster.** 1998. Influenza A virus lacking the NS1 gene replicated in interferon-deficient systems. Virology **252:**324–330.
11. **Hardwick, J. M., and P. M. Bolster.** 2003. Bax, along with lipid conspirators, allows cytochrome c to escape mitochondria. Mol. Cell **10:**963–965.
12. **Hinshaw, V. S., C. W. Olsen, N. Dybdahl-Sissoko, and D. Evans.** 1994. Apoptosis: a mechanism of cell killing by influenza A and B viruses. J. Virol. **68:**3667–3673.
13. **Jaattela, M., C. Cande, and G. Kroemer.** 2004. Lysosomes and mitochondria in the commitment to apoptosis: a potential role for cathepsin D and AIF. Cell Death Differ. **11:**135–136.
14. **Karbowski, M., and R. J. Youle.** 2003. Dynamics of mitochondrial morphology in healthy cells and during apoptosis. Cell Death Differ. **10:**870–880.
15. **Kochs, G., A. Garcia-Sastre, and L. Martinez-Sobrido.** 2007. Multiple anti-interferon actions of the influenza A virus NS1 protein. J. Virol. **81:**7011–7021.
16. **Kroemer, G., L. Galluzzi, and C. Brenner.** 2007. Mitochondrial membrane permeabilization in cell death. Physiol. Rev. **87:**99–163.
17. **Li, L., J. Backer, A. S. K. Wong, E. L. Schwanke, B. G. Stewart, and M. Pasdar.** 2003. BCL-2 expression decreases cadherin-mediated cell-cell adhesion. J. Cell Sci. **116:**3687–3700.
18. **Li, S., J. Y. Min, R. M. Krug, and G. C. Sen.** 2006. Binding of the influenza A virus NS1 protein to PKR mediates the inhibition of its activation by either PACT or double-stranded RNA. Virology **349:**13–31.
19. **Lowy, R. J.** 2003. Influenza virus induction of apoptosis by intrinsic and extrinsic mechanisms. Int. Rev. Immunol. **22:**425–449.
20. **Ludwig, S., O. Planz, S. Pleschka, and T. Wolff.** 2003. Influenza virus induced signaling cascades: targets for antiviral therapy. Trends Mol. Med. **9:**46–52.
21. **Ludwig, S., S. Pleschka, O. Planz, and T. Wolff.** 2006. Ringing the alarm bells: signaling and apoptosis in influenza-infected cells. Cell. Microbiol. **8:**375–386.
22. **McLean, J. E., A. Ruck, A. Shirazian, F. Pooyaei-Mehr, and Z. F. Zakeri.** 2008. Viral manipulation of cell death. Curr. Pharm. Des. **14:**198–220.
23. **Mori, I., T. Komatsu, K. Takeuchi, K. Nakakuki, M. Sudo, and Y. Kimura.** 1995. In vivo induction of apoptosis by influenza virus. J. Gen. Virol. **76:**2869–2873.
24. **Muñoz-Jordán, J., M. Laurent-Rolle, J. Ashour, L. Martínez-Sobrido, M. Ashok, W. Lipkin, and A. García-Sastre.** 2005. Inhibition of alpha/beta interferon signaling by the NS4B protein of flaviviruses. J. Virol. **79:**8004–8013.
25. **Munoz-Jordan, J. G., G. Sanchez-Burgos, M. Laurent-Rolle, and A. Garcia-Sastre.** 2003. Inhibition of interferon signaling by dengue virus. Proc. Natl. Acad. Sci. USA **100:**14333–14338.
26. **Nencioni, L., G. DeChiara, R. Sgarbanti, D. Amatore, K. Aquilano, M. Marcocci, A. Serafino, M. Torcia, F. Cozzolino, M. R. Ciriolo, E. Garaci, and A. T. Palamara.** 2009. Bcl-2 expression and p38MAPK activity in cells infected with influenza A virus: impact on virally induced apoptosis and viral replication. J. Biol. Chem. **284:**16004–16015.
27. **Neumar, R. W., Y. A. Xu, H. Gada, R. P. Guttman, and R. Siman.** 2003. Cross-talk between calpain and caspase proteolytic systems during neuronal apoptosis. J. Biol. Chem. **278:**14162–14167.
28. **Nichols, J. E., J. A. Niles, and N. J. Roberts, Jr.** 2001. Human lymphocyte apoptosis after exposure to influenza A virus. J. Virol. **75:**5921–5929.
29. **Olsen, C. W., J. C. Kehren, N. R. Dybdahl-Sissoko, and V. S. Hinshaw.** 1996. BCL-2 alters influenza virus yield, spread, and hemagglutinin glycosylation. J. Virol. **70:**663–666.
30. **Park, M.-S., M. L. Shaw, J. Muñoz-Jordan, J. Cros, T. Nakaya, N. Bouvier, P. Palese, A. García-Sastre, and C. Basler.** 2003. Newcastle disease virus (NDV)-based assay demonstrates interferon-antagonist activity for NDV V protein and the Nipah virus V, W, and C proteins. J. Virol. **77:**1501–1511.
31. **Ramphal, R., P. M. Small, J. W. Shands, Jr., W. Fischlschweiger, and P. A. Small, Jr.** 1980. Adherence of *Pseudomonas aeruginosa* to tracheal cells injured by influenza infection or by endotracheal intubation. Infect. Immun. **27:**614–619.
32. **Ruiz-Vela, A., G. Gonzáles de Buitrago, and C. Martínez-A.** 1999. Implication of calpain in caspase activation during B cell clonal deletion. EMBO J. **18:**4988–4998.
33. **Schultz-Cherry, S., R. M. Krug, and V. S. Hinshaw.** 1998. Induction of apoptosis by influenza virus. Semin. Virol. **8:**491–495.
34. **Schultz-Cherry, S., N. Dybdahl-Sissoko, G. Neumann, Y. Kawaoka, and V. Hinshaw.** 2001. Influenza virus NS1 protein induces apoptosis in cultured cells. J. Virol. **75:**7875–7881.
35. **Seo, S. H., E. Hoffmann, and R. G. Webster.** 2004. The NS1 gene of H5N1 influenza viruses circumvents the host anti-viral cytokine responses. Virus Res. **103:**107–113.
36. **Takizawa, T., R. Fukuda, T. Miyawaki, K. Ohashi, and Y. Nakanishi.** 1995. Activation of the apoptotic Fas antigen-encoding gene upon influenza virus infection involving spontaneously produced beta-interferon. Virology **209:**288–296.
37. **Takizawa, T., C. Tatematsu, K. Ohashi, and Y. Nakanishi.** 1999. Recruitment of apoptotic cysteine proteases (caspases) in influenza virus-induced cell death. Microbiol. Immunol. **43:**245–252.
38. **Uchide, N., and H. Toyoda.** 2007. Molecular pathogenesis of influenza virus infection: apoptosis induction and macrophage activation, p. 91–128. *In* A. R. Demasi (ed.), Cellular signaling and apoptosis research. Nova Science Publishers, Inc., Haupauge, NY.
39. **Wang, X., M. Li, H. Zhang, T. Muster, P. Palese, A. A. Beg, and A. García-Sastre.** 2000. Influenza A virus NS1 protein prevents activation of NF-κB and induction of alpha/beta interferon. J. Virol. **74:**11566–11573.
40. **Wei, M. C., X. Zong, E. H. Y. Cheng, T. Lindsten, V. Panoutsakopoulou, A. J. Ross, K. A. Roth, G. R. MacGregor, C. B. Thompson, and S. J. Korsmeyer.** 2001. Proapoptotic Bax and Bak: a requisite gateway to mitochondrial dysfunction and death. Science **292:**727–730.
41. **Wurzer, W.** 2003. Caspase 3 activation is essential for efficient influenza virus propagation. EMBO J. **22:**2717–2728.
42. **Wurzer, W. J., C. Ehrhardt, S. Pleschka, F. Berberich-Siebelt, T. Wolff, H. Walczak, O. Planz, and S. Ludwig.** 2004. NF-kappa-beta dependent induction of tumor necrosis factor-related apoptosis inducing ligand (TRAIL) and Fas/FasL is crucial for efficient influenza virus propagation. J. Biol. Chem. **279:**30931–30937.
43. **Zamarin, D., A. Garcia-Sastre, X. Xiao, R. Wang, and P. Palese.** 2005. Influenza virus PB1-F2 protein induces cell death through mitochondrial ANT3 and VDAC1. PLoS Pathog. **1:**e4.
44. **Zamarin, D., M. B. Ortigoza, and P. Palese.** 2006. Influenza A virus PB1-F2 protein contributes to viral pathogenesis in mice. J. Virol. **80:**7976–7983.
45. **Zhirnov, O., T. E. Konakova, W. Garten, and H. D. Klenk.** 1999. Caspase-dependent N-terminal cleavage of influenza virus nucleocapsid protein in infected cells. J. Virol. **73:**10158–10163.
46. **Zhirnov, O. P., T. E. Konakova, T. Wolff, and H.-D. Klenk.** 2002. NS1 protein of influenza A virus down-regulates apoptosis. J. Virol. **76:**1617–1625.